

Melting in multilayer adsorbed films

M. S. Pettersen, M. J. Lysek, and D. L. Goodstein

Condensed Matter Physics 114-36, California Institute of Technology, Pasadena, California 91125

(Received 19 July 1988; revised manuscript received 24 April 1989)

We present both an improved model and new experimental data concerning the problem of melting in multilayer adsorbed films. The model treats in a mutually consistent manner all interfaces in a stratified film. This results in the prediction of substrate freezing, a phenomenon thermodynamically analogous to surface melting. We also compare the free energies of stratified films to those of homogeneous films. This leads to an orderly classification of multilayer phase diagrams in the vicinity of the bulk triple point. The results of the model are compared with the experimentally known systems. Of these, only methane/graphite exhibits melting from homogeneous solid to homogeneous liquid in multilayer films. The systems Ne/graphite and Ar/graphite, studied by Zhu and Dash, exhibit surface melting and substrate freezing instead. We observe experimentally, by means of pulsed nuclear magnetic resonance, that melting in methane adsorbed on graphite extends below the film thickness at which the latent heat of melting is known to vanish. The multilayer melting curve in this system is a first-order prewetting transition, extending from triple-point dewetting at bulk coexistence down to a critical point where the latent heat vanishes at about four layers, and apparently extending to thinner films as a higher-order, two-dimensional phase transition. It would therefore seem that methane/graphite is an ideal system in which to study the evolution of melting from two dimensions to three dimensions.

I. INTRODUCTION

The thermodynamic behavior of multilayer adsorbed films provides an unusual means to study the phenomenon of melting, by varying the dimensionality of the system. If both solid and liquid phases wet the substrate, the possibility exists of following the melting transition from the monolayer, two-dimensional (2D) regime all the way to bulk (3D) behavior. In many systems, it is found that the solid phase does not wet the substrate, and they are therefore unsuitable for this kind of study.¹ However, a few systems have been found in which both solid and liquid phases do appear to wet the substrate or at least to grow very thick films.²⁻⁷ Recent studies of these systems have raised a considerable number of interesting issues.

The first system to be surveyed experimentally for this purpose was methane on graphite.^{3,4} More recently, neon and argon on graphite and methane on MgO have been added to the list.⁵⁻⁷ The methane, neon, and argon studies on graphite all yield evidence that a roughening transition exists in the bulk solid phase, and all reveal a latent heat of melting that diminishes as the film becomes thinner, vanishing entirely at three and one-half to four layers. However, in the methane/graphite case melting appears to involve coexistence of solid and liquid films on different parts of the substrate giving rise to a new kind of phase transition known as triple-point dewetting. In the neon and argon/graphite cases and in methane/MgO the film is thought to become stratified instead, with melting starting at the surface and progressing through the film as the temperature is raised. This behavior is taken as evidence that surface melting occurs in the solid phase of the bulk adsorbate.

In the thick-film limit, it is possible to analyze the behavior of these systems by means of thermodynamically dependable models. Indeed, each of the types of behavior described above had been anticipated in advance of their experimental verification.⁸ However, these analyses have not heretofore been applied to experimental data in a fully consistent way. The analyses employed by previous authors (ourselves included) have been lacking in two important ways. For one thing, the film-substrate interface has not been considered in a manner consistent with the treatment of the film-vapor interface. When this is done, "substrate freezing," a phenomenon symmetric with surface melting, is introduced, and expectations for the behavior of the film are altered in a number of important ways. Second, each set of authors has analyzed their data using a model that assumed the conclusion (triple-point dewetting or surface melting of the film) at which they ultimately arrived. A proper analysis must include a comparison of the free energies of stratified (liquid on top of solid) and homogeneous (solid or liquid) films, thus allowing either result to occur. When this job is done, we find an orderly classification of possible surface phase diagrams in the thick-film limit, and the thermodynamic signatures of each type of behavior. These results suggest a possible reinterpretation of some of the existing experimental data, and help to clarify the questions that may be resolved by further experiment.

In thinner films (i.e., from one to four layers), few predictions exist, and the vanishing latent heat has made the melting transition impossible to follow further by means of thermodynamic measurements. However, this is precisely where the physics becomes most interesting. For example, it is known that 2D solid films become unstable with respect to melting by dislocation unbinding and may

in some cases melt by this mechanism, first proposed by Kosterlitz and Thouless.⁹ On the other hand, melting in 3D is not well understood, and theoretical attempts to extend the Kosterlitz-Thouless mechanism to 3D have not been successful. Experimental evidence connecting 2D melting to 3D melting would therefore be of considerable interest.

To pursue this problem, we present new experimental data, in which pulsed nuclear magnetic resonance (NMR) measurements are used to follow the melting transition to regions below the thickness where the latent heat vanishes in methane/graphite. These data are interpreted to show that melting does persist, with zero latent heat, in the region one to four molecular layers, but is not to be found below one layer. We are able to conclude, therefore, that the first-order melting (and prewetting) transition ends at about four layers in a critical point, with melting continuing to thinner films probably as a higher-order phase transition. Unfortunately, the temperature resolution in these measurements is not good enough to allow us to follow the trajectory of the phase transition and discover where it ends. The NMR data also afford confirming evidence that surface melting of the film can be ruled out in methane/graphite, and indicate that the roughening transition is accompanied by an increase in surface mobility.

In Sec. II of this paper, we present our new thermodynamic analysis, and compare the results with existing data. Our experimental results are presented and interpreted in Sec. III, and we review and discuss our conclusions in Sec. IV.

II. THERMODYNAMICS

In a previous publication,⁴ we presented a complete thermodynamic model of melting in a system of homogeneous, unstratified films. The model assumes that the adsorbate can be pictured as an incompressible bulk continuum phase, of density ρ_i , so the surface excess density or coverage n_i is related to the film thickness z_i by $n_i = (\rho_i - \rho_g)z_i$, where the subscript i indicates the phase of the film, which may be either liquid or solid, and ρ_g is a small correction for the amount of gas displaced by the film. The equation of state for the film is taken to be the Frenkel-Halsey-Hill¹⁰ (FHH) isotherm, $\mu - \mu_i(T) = -\Delta C_3^{i\omega} / z_i^3$, where $\mu_i(T)$ is the chemical potential of the bulk phase i at coexistence with its vapor, and $\Delta C_3^{i\omega} = C_3^{(\omega)} - C_3^{(i)}$, the difference between the coefficients of the van der Waals potentials of a half-space of substrate and adsorbate, respectively. From these two assumptions, we derived the Landau potential excess for each phase,

$$\frac{\Omega^i}{A} = \frac{3}{2} \frac{\rho_i \Delta C_3^{i\omega}}{z_i^2} + \sigma_{ig} + \sigma_{i\omega}, \quad (1)$$

or in terms of its proper variables,

$$\frac{\Omega^i}{A} = \frac{3}{2} \rho_i (\Delta C_3^{i\omega})^{1/3} [\mu_i(T) - \mu]^{2/3} + \sigma_{ig} + \sigma_{i\omega},$$

where the σ 's are the surface tensions of an infinitely

thick slab of the adsorbate with its vapor and the substrate, respectively. (Our previous work, however, neglected the slight distinction between $\Delta C_3^{l\omega}$ and $\Delta C_3^{s\omega}$.)

The transition between the two homogeneous phases will occur when the Landau potentials are equal, $\Omega^l = \Omega^s$, resulting in the melting curve

$$\rho_s (\Delta C_3^{s\omega})^{1/3} [\mu_s(T) - \mu]^{2/3} - \rho_l (\Delta C_3^{l\omega})^{1/3} [\mu_l(T) - \mu]^{2/3} = -\frac{2}{3} \delta,$$

where δ is the difference of surface tensions,

$$\delta = \sigma_{sg} + \sigma_{s\omega} - \sigma_{lg} - \sigma_{l\omega}.$$

Pandit and Fisher⁸ point out that, in general, one expects $\delta \neq 0$. This results in the conclusion that the melting transition in the film does not approach the bulk triple point, but (for the case $\delta > 0$) the melting curve intersects the bulk solid coexistence curve at a temperature

$$T_w = T_l - \frac{1}{\alpha} \left[\frac{2}{3} \frac{\delta}{\rho_l (\Delta C_3^{l\omega})^{1/3}} \right]^{3/2},$$

and with a slope

$$d(\mu_s - \mu) / dT \propto (T_w - T)^{1/2},$$

where α is the difference in slopes

$$\alpha = (d\mu_s / dT - d\mu_l / dT) |_{T_l}$$

and is related to the bulk latent heat of melting per molecule L by $\alpha \simeq L / T_l$. Thus, for $\delta > 0$, the surface tension favors stability of the liquid phase below T_l . Furthermore, between T_w and T_l , a liquid film can coexist with bulk solid, but a solid film is unstable. Hence, a film warming up through T_w must convert any film in the solid phase into bulk crystallites—a dewetting transition. Finally, the asymptotic form of the melting curve at T_w , together with FHH, implies that for a film of coverage n , the temperature T_p at which melting begins obeys $(T_w - T_p) \propto 1/n^2$. These predictions were found to be obeyed by methane adsorbed on graphite. In other words, even though solid and liquid methane each individually wet the graphite substrate, the relative values of the various surface tensions cause a first-order dewetting transition at T_w , and the multilayer melting curve itself is an example (the only example we are aware of) of a first-order "prewetting" transition.

More recently, experiments by Zhu and Dash^{5,6} and Bienfait *et al.*⁷ have indicated that in neon and argon on graphite and methane on MgO, the film melts by forming a liquid layer at the solid-gas interface. Thermodynamically, the idea is that if $\sigma_{sg} \geq \sigma_{sl} + \sigma_{lg}$, then the liquid wets the bulk solid; and near the triple point, where the free-energy densities of liquid and solid are nearly equal, the extra energy cost of making a thin layer of liquid at the surface may be more than compensated for by the decrease in surface tension obtained by replacing the solid-gas interface by two interfaces of lower total surface tension. (Thus, by the term σ_{sg} in the inequality we denote the energy of the metastable bare solid-gas interface.)

Then as T_i is approached from below, the surface layer of liquid will grow until it consumes the solid. This phenomenon is known as surface melting. If it is assumed that the growth of the liquid on the solid surface can be described by the FHH equation, then when this occurs in an adsorbed film, the heat capacity will obey the power law $C_N \propto (T_i - T)^{-4/3}$ and isosteric melting will terminate at a temperature T_p given by $T_i - T_p = \Delta C_3^{ls} \rho_l^3 / \alpha n^3$ for each film thickness. Since this prediction is independent of the substrate, it might appear that there is a contradiction between the observation of triple-point dewetting in methane/graphite and the observation of surface melting in methane/MgO. We shall reexamine this point below. The model presented by Zhu and Dash is simple and physically appealing, but it neglects an important interaction between the liquid-solid interface and the solid-substrate interface. In other words, in a horizontally stratified film, as sketched in Fig. 1, there are three interfaces that must be treated in a mutually consistent manner. Such a calculation has been carried out by An and Schick,¹¹ on a spin model that exhibits a triple point at zero temperature under the influence of various fields. In this paper, we present a model more transparently applicable to solids, liquids, and gases at finite temperature, using the slab method of deGennes.¹²

We wish to add up all the excess free energy in the system due to the fact that it is inhomogeneous, given the assumption that the medium is at each point locally bulk-like and in equilibrium. One contribution to this energy arises from the presence of condensed phases in the region of the phase diagram where the state of lowest free energy is the vapor. Since the Gibbs free energy per particle is equal to the chemical potential, the extra energy cost per area of forming the wrong phase may be written $(\rho_i - \rho_g)[\mu_i(T) - \mu]z_i$, where z_i is the thickness of the stratum of the film in phase i . The correction to the Landau potential is the same as the correction to the Gibbs free energy.¹³ Each molecule in the system in addition feels a potential $\Delta\phi(r)$, where the external field $\Delta\phi$ is the perturbation of the local van der Waals potential due to

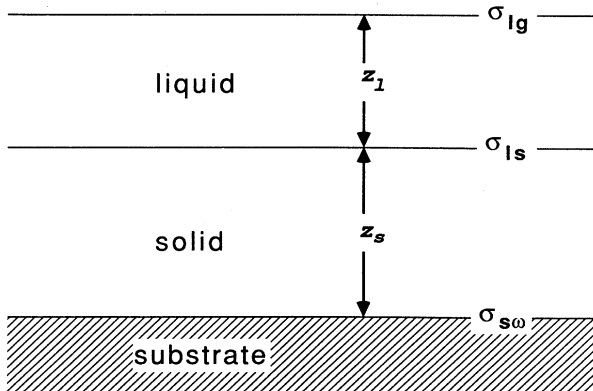


FIG. 1. Schematic cross section of a stratified film.

the fact that far away the medium is replaced by some other phase (or substrate). The interaction between two semi-infinite media is subsumed in the surface tension; then the integrals that appear as corrections for the finite thickness of the film depend only on the well-known asymptotic tail of the van der Waals potential and on the density of the film far from the interface. With the approximation that the potential of a half-space of some medium is proportional to its density, the coefficients can be computed, and the resulting surface excess Landau potential is found to be

$$\frac{\Omega^{sm}}{A} = (\rho_s - \rho_l) \frac{\Delta C_3^{s\omega}}{2z_s^2} + \rho_l \frac{\Delta C_3^{ls}}{2z_l^2} + \rho_l \frac{\Delta C_3^{s\omega}}{2(z_s + z_l)^2} - \rho_l [\mu - \mu_l(T)]z_l - \rho_s [\mu - \mu_s(T)]z_s + \sigma_{s\omega} + \sigma_{sl} + \sigma_{lg},$$

where here and henceforth we are subsuming the terms ρ_g into reduced densities, $\rho_i - \rho_g \rightarrow \rho_i$. The simplest way to turn Ω^{sm} into an equation of state is to observe that the equilibrium values of z_l and z_s will minimize Ω^{sm} for fixed μ . Thus, the following coupled equations relate (z_l, z_s) to (μ, T) :

$$\rho_l [\mu - \mu_l(T)] = -\rho_l \left[\frac{\Delta C_3^{ls}}{z_l^3} + \frac{\Delta C_3^{s\omega}}{(z_s + z_l)^3} \right], \quad (2a)$$

$$\rho_s [\mu - \mu_s(T)] = - \left[(\rho_s - \rho_l) \frac{\Delta C_3^{s\omega}}{z_s^3} + \rho_l \frac{\Delta C_3^{s\omega}}{(z_s + z_l)^3} \right]. \quad (2b)$$

This is the equation of state, the analog of the FHH equation, for a stratified film. Substituting into the previous equation, we find that Ω^{sm} simplifies to

$$\frac{\Omega^{sm}}{A} = \frac{3}{2} \left[(\rho_s - \rho_l) \frac{\Delta C_3^{s\omega}}{z_s^2} + \rho_l \frac{\Delta C_3^{ls}}{z_l^2} + \rho_l \frac{\Delta C_3^{s\omega}}{(z_s + z_l)^2} \right] + \sigma_{s\omega} + \sigma_{sl} + \sigma_{lg}. \quad (3)$$

In the limit that $z_s \rightarrow \infty$, the model should reduce to one of a homogeneous liquid film, with the solid in the place of the substrate. Indeed we find that the Landau potential in Eq. (3) reduces to Eq. (1), and Eq. (2) reduces to the FHH equation, thus confirming our confidence in our procedure. To get Ω^{sm} in terms of its proper variables, Eqs. 2(a) and 2(b) must be solved numerically for z_l and z_s in terms of μ and T . The new model differs from that of Zhu and Dash in that Eqs. 2(a) and 2(b) imply that the substrate stabilizes an underlayer of solid above the triple-point temperature.^{8,11} This phenomenon in the film is related to a phase transition of the bulk liquid-substrate interface, in which a layer of solid forms at the substrate for $T > T_i$, analogous to surface melting at the solid-gas interface at $T < T_i$. In both cases, the phenomenon is caused by a balance of surface tensions. Therefore, it seems natural to call this transition "substrate freezing." We remark that this prediction differs from a similar one made by Krim and Dash¹⁴ in that the stress at the liquid-solid interface is not constrained to

equal the bulk melting pressure.

We can find the heat-capacity signature of surface melting in this model by solving Eqs. 2(a) and 2(b) for (z_l, z_s) as a function of T with $n = \rho_l z_l + \rho_s z_s$ held constant. The heat capacity is mostly due to the conversion of solid to liquid as the liquid-solid interface moves through the film, so $C_N \sim \partial z_l / \partial T$. The resulting heat-capacity curves are shown in Fig. 2 for a variety of film thicknesses using coefficients typical of the systems being studied. We observe that the peaks extend above the triple point, and that they become broader and smaller as the film becomes thinner. The $1/z^2$ terms in the Landau potential behave like repulsive forces between the interfaces, as noted by deGennes.¹² For very thin films, the solid-liquid interface is essentially pinned by these forces at the middle of the film, resulting in the broadening of the transition. A small amount of the wrong phase remains even when the temperature is far from T_t . The heat capacity in this model clearly differs from the power law $C_N \propto (T_t - T)^{-4/3}$ derived from the model of Zhu and Dash; however, it turns out to be a good approximation that $C_N \propto (T_p - T)^{-4/3}$ below T_p , where T_p is the temperature of the heat-capacity peak. Because z_l and z_s appear in Eqs. 2(a) and 2(b) only in terms of degree -3 , the solutions scale, and the peak of the heat-capacity curve varies with thickness as $T_t - T_p \propto n^{-3}$. Both of these results are consistent with the experimental observation on Ne/graphite and Ar/graphite reported by Zhu and Dash, but disagree with the observed behavior of methane/graphite, confirming our earlier conclusion that methane/graphite does not form a stratified film.

An analysis of the methane heat-capacity data shows no evidence of power-law dependence below the peak temperature. Figure 3 shows a log-log plot of C versus $T_0 - T$ for an 18.3 layer film. On the left, T_0 is chosen to

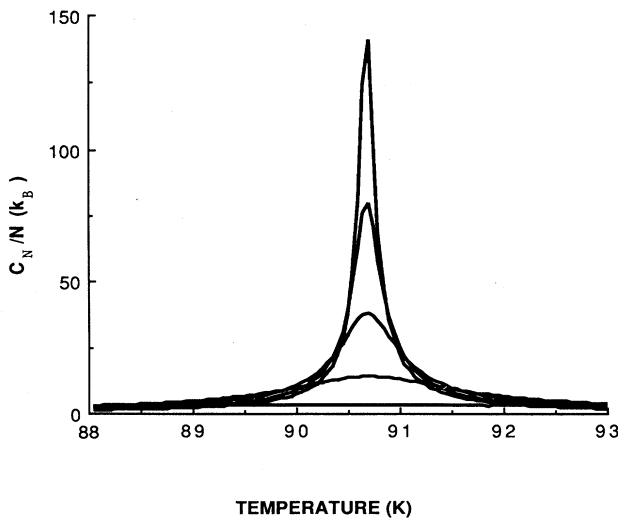


FIG. 2. Predicted heat-capacity signal of melting of a stratified film for coverages of 10, 8, 6, 4, and 2 layers (top to bottom).

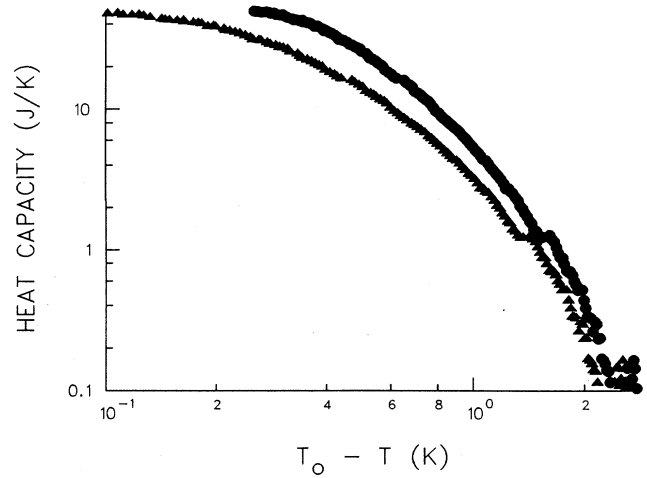


FIG. 3. Rising slope of experimentally measured heat capacity of methane/graphite shows no power-law dependence. Circles, $T_0 = 90.66$ K; triangles, $T_0 = 90.48$ K.

be 90.48 K, the triple-point dewetting temperature. On the right, T_0 is 90.66 K, the methane triple point. (We remark that these temperatures were independently measured in the experiment of Ref. 4.) For both cases there is no sign of a power law. Examining the data by plotting $C^{-3/4}$ versus T in order to test for $C \propto (T_0 - T)^{-4/3}$ for any T_0 also indicates no such behavior in these data. In addition, as pointed out above, the peak temperatures obey $T_w - T_p \propto n^{-2}$ and do not obey $T_t - T_p \propto n^{-3}$. These observations confirm that the heat-capacity peaks in the methane/graphite system are due to the melting of a homogeneous film, associated with triple-point dewetting, and not to the behavior of a stratified film.

Let us examine the value of the coefficient of proportionality $\xi \equiv n^3(T_t - T_p)$ for cases where melting does proceed through stratification. In the simpler model, $\xi = \Delta C_3^l \rho_l^3 / \alpha$. Exact numerical results for the present model are shown in Table I, but for convenience of calculation, we also present an evaluation of ξ to first order in the small quantity $\Delta\rho = \rho_s - \rho_l$,

$$\xi = \frac{\rho^3}{\alpha} \left\{ \Delta C_3^l (x+1)^3 - \Delta C_3^{s\omega} \frac{\Delta\rho}{\rho} \left[\left(\frac{x+1}{x} \right)^3 - 1 \right] \right\},$$

where $x = (\Delta C_3^{s\omega} \Delta\rho / \Delta C_3^l \rho)^{1/5}$ and $\rho = (\rho_s + \rho_l)/2$. (The values of ΔC_3 are computed from the model of Vidali and

TABLE I. Values of the coefficient ξ . gr signifies graphite.

ξ (mK \AA^{-6})	Ne/gr	Ar/gr	CH ₄ /gr
Old model	3.1	3.5	2.0
New model	-34	-11	-3.6
New model (linearized)	-24	-4.9	-1.7
Experimental	134 ^a	67 ^b	

^aReference 5.

^bReference 6.

Cole.¹⁵) The linearized calculation clearly shows that the sign of ζ is the result of competing effects, and so depends sensitively on the values of ΔC_3 used. Our calculations indicate that the sign of the temperature shift for Ne, Ar, and methane on graphite is opposite to that predicted by the simpler model. Finally, we also show in the table measurements of ζ extracted from the data of Zhu and Dash^{5,6} for Ne and Ar. The measurements obviously disagree with both models of surface melting of the film. The significance of this disagreement is not clear to us. By contrast, the observed value of $n^2(T_W - T_p)$ reported in Ref. 4 for methane is in excellent agreement with the model of Vidali and Cole.

Finally, we address the question of whether or not the stratified phase is stable with respect to the formation of homogeneous film phases, by comparing the Landau potentials. The results will depend on two parameters,

$$\delta = \sigma_{sg} + \sigma_{s\omega} - \sigma_{lg} - \sigma_{l\omega}$$

and

$$\delta' = \sigma_{sg} - \sigma_{lg} - \sigma_{sl}.$$

The first parameter, δ , measures the difference in surface tension between films of liquid and solid; and the second, δ' , measures the degree to which surface melting is favored in the bulk solid. Through δ , melting behavior of the adsorbed film can depend on the substrate. Thus, it is possible to have first-order melting between homogeneous phases and a triple-point dewetting transition in one system (methane/graphite), and melting by stratification for the same adsorbate on another substrate (methane/MgO).

The following general rules determine the topology of the phase diagram (for the case $\rho_s > \rho_l$). The sign of δ' governs whether the transition between homogeneous solid and stratified phases occurs above or below the triple point; and the sign of $\delta - \delta'$, whether the transition between homogeneous liquid and stratified phases occurs above or below the triple point. If $\delta > 0$ and

$$(\Delta C_3^{ls} / \Delta C_3^{lw})^{1/3} \delta > \delta',$$

or $\delta < 0$ and

$$[(1 - \rho_l / \rho_s)^{1/3} - 1] |\delta| > \delta',$$

then stratification is suppressed, and the sign of δ determines the location of the solid-liquid transition. For $\delta = 0.21 \text{ K/\AA}^2$ (the experimentally determined value for methane/graphite from Ref. 4) and any value of $\delta' \leq 0.07 \text{ K/\AA}^2$ the stratified phase of the film is never stable, despite the fact that $\delta' \geq 0$ is the condition for surface melting in the bulk; the resulting phase diagram shown in Fig. 4(a) is the same as that proposed for methane/graphite in Ref. 4. Conversely, for the values $\delta = -0.5 \text{ K/\AA}^2$ and $\delta' = -0.1 \text{ K/\AA}^2$, used to generate Fig. 4(b), a stratified phase occurs in the film, even though for negative values of δ' surface melting does not occur in the bulk.

In Fig. 4(c), the stratified phase is allowed both above and below T_t , and the heat capacity in the vicinity of the triple point resembles the curves shown in Fig. 2. However, all of the phase boundaries shown in Fig. 4 mark

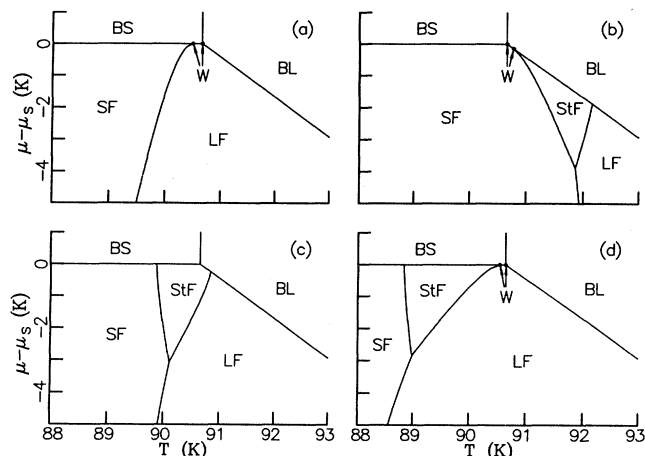


FIG. 4. Hypothetical phase diagrams. BS denotes bulk solid, BL denotes bulk liquid, SF denotes solid film, LF denotes liquid film, StF denotes stratified film; between the points marked W , nonwetting occurs. (a) $\delta = 0.21 \text{ K/\AA}^2$, $\delta' \leq 0.07 \text{ K/\AA}^2$; (b) $\delta = -0.5 \text{ K/\AA}^2$, $\delta' = -0.1 \text{ K/\AA}^2$; (c) $\delta = 0.1 \text{ K/\AA}^2$, $\delta' = 0.2 \text{ K/\AA}^2$; (d) $\delta = 0.45 \text{ K/\AA}^2$, $\delta' = 0.35 \text{ K/\AA}^2$.

first-order transitions, and so the slab model predicts heat-capacity signals when the film enters or leaves the stratified region of the diagram, in addition to the peak near the triple point. This kind of phase diagram was also obtained by An and Schick,¹¹ who also considered layering transitions that cannot occur in our model.

Figure 4(d) resembles 4(b) except that the stratified phase is stable only below T_t . We remark that the liquid bulk phase cannot wet the substrate below T_t , nor the solid above it, so that Figs. 4(a), 4(b), and 4(d) all have narrow regions of nonwetting between the points marked W . Figures 4(b) and 4(d) illustrate that triple-point dewetting and stratification may be exhibited by the same system. Phase diagrams like those of Fig. 4 were also proposed by Pandit and Fisher.⁸ Otherwise, however, the possibility of first-order transitions from a homogeneous phase to a stratified phase does not appear to have been fully appreciated.

According to our model, the stratified state is never favored for very thin films, because of the high-energy cost of the repulsion between the interfaces. Thus, if stratification occurs there must be a triple point between the adsorbed solid, adsorbed liquid, and stratified phases. However, the predictions of the model cannot be regarded as dependable in the thin-film limit.

Let us summarize briefly the results we have obtained in this section.

(1) First-order melting between homogeneous phases of the film is possible even if surface melting occurs in the bulk, and conversely, melting by stratification may occur in a film even if surface melting does not occur in the bulk.

(2) The balance of surface tensions may cause a liquid-substrate interface to freeze at $T > T_t$, in analogy to the possible melting of the solid-gas interface at $T < T_t$. The

latter is called surface melting; we have suggested that the former be called substrate freezing.

(3) Triple-point dewetting and stratification can occur in the same system, as in Figs. 4(b) and 4(d). In general, the model predicts that stratification should be accompanied by first-order phase transitions, as in Figs. 4(b)–4(d).

(4) When stratification does occur in a (thick) film, the thicknesses of the solid and liquid strata are given by Eqs. (2a) and (2b), which play a role similar to that of the FHH equation for a homogeneous film.

III. EXPERIMENTAL RESULTS AND DISCUSSION

In the methane/graphite system, unlike Ne/graphite and Ar/graphite, the vanishing latent heat of melting in thin films is not predicted by our model. Therefore, there is new physics to be learned in this region. In order to study the behavior of the melting transition, and to investigate the dynamical behavior of the film in the range of coverage < 4 layers, where the latent heat vanishes, we have made an NMR survey of the system of methane on graphite from 70 to 105 K in temperature and 1 to 50 layers in coverage. Our data were taken with a 30 MHz pulsed NMR spectrometer based on a design by Clark.¹⁶ The Pyrex sample cell contained 1.4 g of Grafoil. (Grafoil is a registered trademark of the Union Carbide Corp.) The thermometer was a carbon glass resistor from Lakeshore Cryogenics. While the data were collected, the external environment of the cell was made to drift in temperature at a rate of 10–15 K/8 h. The amount of hysteresis present in experiments performed on bulk methane, in the absence of Grafoil, indicates that the thermometer followed the cell temperature to better than 1 K. Because of the inhomogeneity of the rf field H_1 caused by the electrical conductivity of the Grafoil substrate, no attempt was made to perform Carr-Purcell pulse sequences,¹⁷ and T_2 was determined from simple spin echoes.

Data for thick films have been presented in a separate paper.¹⁸ Those data are interpreted to show that both solid and liquid methane wet graphite to a thickness of at least 50 layers and that the dynamical properties of thick films are much like those of the corresponding bulk phases.

Values of T_2 , for films of 17 layers and less, are shown in Figs. 5 and 6. Figure 5(a) also shows the data of deWit and Bloom¹⁹ for bulk solid methane. The intrinsic T_2 of bulk liquid methane has never successfully been measured. However, bulk liquid is presumably in the regime of extreme motional narrowing where one expects $T_2 = T_1$, and T_1 is measured to be of the order of several seconds.^{18,20}

In all cases except Fig. 6(d) (for which, see below) the data at low temperature are quite similar to those of bulk solid, where the relaxation mechanism is coupling to diffusive molecular motion in the lattice. At higher temperature, T_2 becomes constant, which we presume to be a characteristic of the melted film, since thermodynamic data show the film to be melted in this region for all

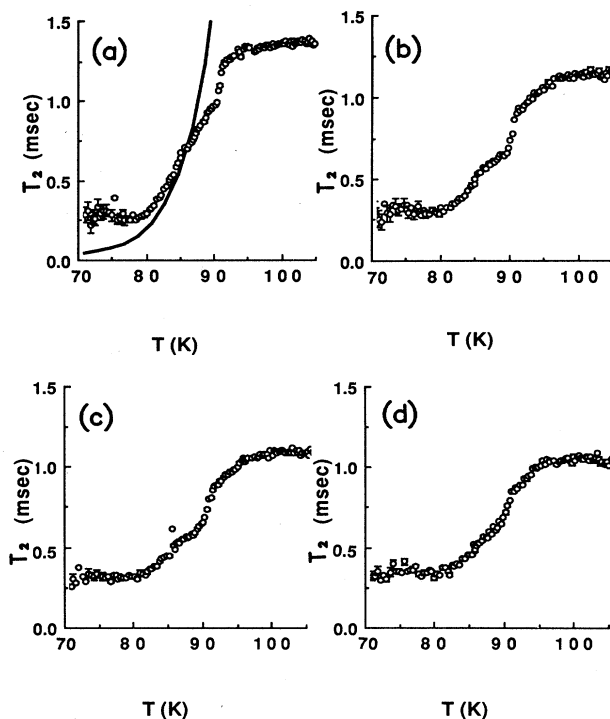


FIG. 5. T_2 for coverages of (a) 17 layers, (b) 13 layers, (c) 10 layers, and (d) 7.4 layers. Solid curve in (a) shows data of deWit and Bloom (Ref. 18).

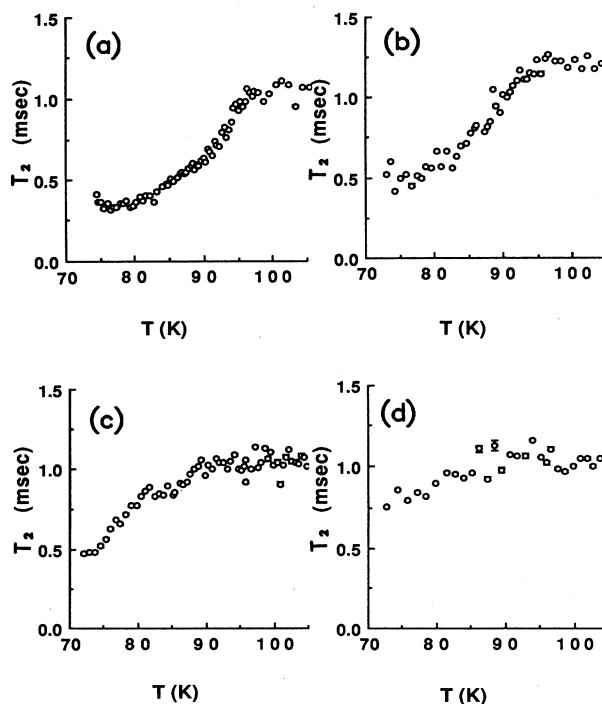


FIG. 6. T_2 for coverages of (a) 4.6 layers, (b) 3.5 layers, (c) 1.8 layers, and (d) 0.87 layers.

thicknesses greater than about four layers. In the thickest films, there is a discernible discontinuity at the melting transition, but the discontinuity is smeared out, even in films as thick as ten layers [Fig. 5(c)]. Guided by the position of the discontinuity in Figs. 5(a) and 5(b), we regard Figs. 5(c), 5(d), 6(a), 6(b), and 6(c) as indicating melting somewhere in the vicinity of 90 K, for films between 1.8 and 10 layers. However, we see no means of extracting from the data with any precision the temperature at which melting occurs in each case.

In our films T_2 is clearly much shorter at high T than is expected in bulk liquid. The explanation, originally offered by Husa,²¹ is based on a model due to Robertson.²² The idea is that the inhomogeneous and anisotropic magnetic susceptibility of Grafoil results in large gradients in the dc magnetic field along the platelets. The spins diffuse back and forth across the platelets, precessing at different rates, losing phase coherence, and the net transverse magnetization M_1 decays because of destructive interference. After the time characteristic of diffusion across the field gradient, a^2/D , the magnetization follows the asymptotic form

$$M_1(t) \propto \exp\left[-\frac{a^4\gamma^2G^2}{120D}t\right], \quad (4)$$

where D is the diffusion constant, γ is the proton gyromagnetic ratio, a is the platelet size, and G is the field gradient. Thus, one observes a pure exponential decay, but with a shortened time constant $T_2^* = 120D/a^4\gamma^2G^2$. This result will hereafter be referred to as the bounded-diffusion model. Because the exponential decay of Eq. (4) cannot be distinguished experimentally from that due to intrinsic relaxation mechanisms, we shall denote both T_2 and T_2^* as T_2 .

For the solid, $a^2/D \geq 2.5$ sec, which is much greater than T_2 . Thus, the magnetization decays before the effects of diffusion across platelets become important, which is why the values of T_2 in solid film agree with the bulk data.

Figures 5(b) and 5(c) show that the discontinuity in T_2 at melting gradually diminishes to a change in slope as the coverage is reduced. This effect probably should not be interpreted as an indication that melting is becoming continuous; in fact, as we have seen, the mechanism relaxing the transverse magnetization is not the same in the solid and liquid phases. More likely, the discontinuity in T_2 , which is small to begin with, is obscured by the effects of substrate inhomogeneity, which are known to broaden phase transitions in adsorbed films by a degree or more in temperature.²³ We have seen in the previous section that the melting curve is very sensitive to the substrate potential and surface tensions, so if there exist imperfections in the surface, there may be points on the substrate where the melting transition takes place at lower or higher temperature than the rest of the surface.

Perhaps the most striking feature of the data shown in Fig. 5 is the weakness of the dependence of T_2 on coverage. Figure 7 shows that for films less than four layers, T_2 increases with decreasing coverage at low temperature. Otherwise, there appears to be remarkably little

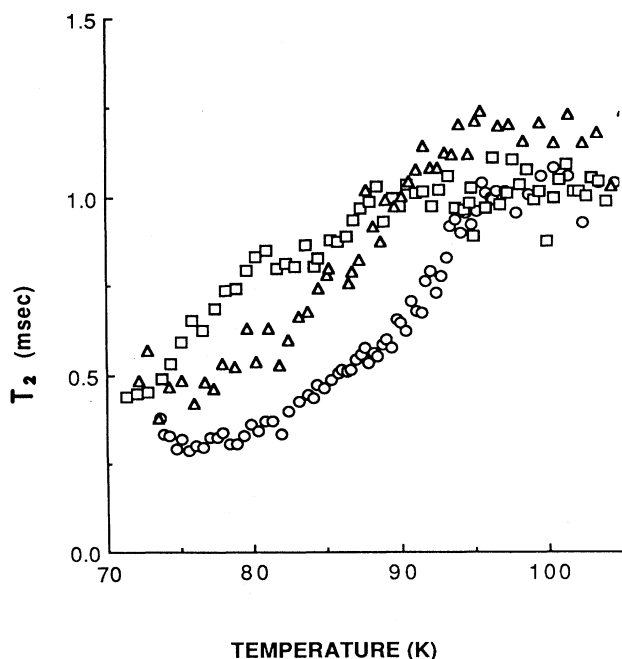


FIG. 7. T_2 for coverages of 4.6 layers (circles), 3.5 layers (triangles), and 1.8 layers (squares) on common scale.

change in the signal with film thickness.

To test the possibility that the data are the result of an instrumental artifact, one run, shown in Fig. 6(d), was made at submonolayer coverage. Quateman and Bretz have observed a change in slope of T_2 versus T at the monolayer triple point, 57 K,²⁴ but the curve should not have any feature near the bulk triple point, and Fig. 6(d) shows that this is indeed the case, confirming that our other data are valid. We conclude that melting persists in films between 1.8 and 4 layers thick, where the latent heat is zero.

Although we have argued above that stratification does not occur in this system, it seems worthwhile to examine the NMR data for evidence of that phenomenon, just as we have done with the thermodynamic data. Let us therefore consider what the NMR signal of a stratified film should look like. For thin films such as we consider here, diffusion would cause rapid exchange of molecules between the liquid and solid strata, so each spin experiences an average relaxation rate which is a weighted average of the individual rates,

$$\frac{1}{T_2} = \frac{x_l}{T_2^l} + \frac{x_s}{T_2^s},$$

where x_l, x_s are the fraction of the film in the two phases. Using the stratification model of the previous section to predict the quantities x_l, x_s as a function of coverage and temperature, we find that at all temperatures, surface melting or substrate freezing should result in an elevation of T_2 with respect to its value in an unstratified film, or with respect to a very thick film where the surface layers

are a negligible fraction of the whole. This is because T_2^s is a rapidly rising function of temperature and crosses T_2^l near the melting transition. Thus, below T_l , $T_2^l > T_2^s$ and the presence of liquid raises T_2 ; while for higher temperatures, $T_2^s > T_2^l$ and the presence of solid raises T_2 . The predicted elevation of T_2 , which is as much as 50%, is not observed at temperatures above T_l , and this corroborates our belief, based on the heat-capacity data, that stratification is not the mechanism of melting in methane on graphite.

As shown in Fig. 7, we do observe an elevation of T_2 in very thin films, at temperatures below T_l . For a thin film one would expect that the geometrical restriction on molecular motion²² would reduce the effect of motional narrowing and therefore shorten T_2 . Instead, in our films of slightly more than one layer, we see an increase, implying that the multilayer films show enhanced mobility with respect to the bulk. This is consistent with the conclusion of the heat-capacity survey of Hamilton³ that around 78 K, solid methane undergoes a roughening transition. In the rough phase, one would expect some dynamic rearrangement of the atoms in the top few layers. However, except for very thin films, this mobile surface region will be a tiny fraction of the film and its mobility will be hard to detect except by surface techniques. These NMR data and the latent heat data of Ref. 4 both suggest that the width of the roughened interface is approximately four layers. The increase in mobility that we have associated here with roughening is at most a factor of 2. By contrast, an increase of several orders of magnitude is observed⁷ in connection with surface melting.

IV. DISCUSSION AND CONCLUSIONS

According to the analysis we have presented here, the phase diagram of the methane/graphite system is that of Fig. 4(a). We propose that the neon and argon/graphite systems have the phase diagram of Fig. 4(c). In the latter cases, our analysis predicts the vanishing latent heat of melting in thin films. In the former case it does not. This is a crucial point, to which we shall return below. The apparent discrepancy between methane/graphite where triple-point dewetting is observed and methane/MgO, where stratification is reported, can be explained by the difference in film-substrate surface tensions, as discussed above.¹¹ In fact, we have shown that stratification in a film does not necessarily mean that surface melting occurs in the bulk, nor does homogeneous melting in a film necessarily mean that surface melting does not occur in the bulk.

The thermodynamic data presented by Zhu and Dash^{5,6} for the neon and argon/graphite systems do indeed exhibit features similar to those of Fig. 4(c). A series of heat-capacity peaks at $0.8 T_l$ could mark the boundary between the solid and surface melted regions of Fig. 4(c). Zhu and Dash interpret the peaks to indicate layer-by-layer condensation, leading to a roughening transition at infinite thickness. Although that interpreta-

tion is different from ours, we note that even in our interpretation the thick-film limit of the solid-stratified film transition could well coincide with a roughening transition. That is because the liquid-gas interface is always rough due to capillary waves.²⁵

In more recent work, Zhu and Dash²⁶ also report heat-capacity peaks extending above T_l , which they interpret as freezing of the film at the substrate interface. In fact, they are able to distinguish separate curves for the freezing of each of the first three layers above the substrate, a result that could not have been predicted by our continuum slab model. However, instead of substrate freezing induced by the balance of surface tensions as in our model, they attribute the effect to freezing caused by hydrostatic pressure, in accordance with the model of Krim and Dash.¹⁴ We believe that our interpretation of substrate freezing is an alternative to their interpretation of pressure induced freezing that is, at least in principle, distinguishable by experiment. Zhu and Dash observe yet another series of heat-capacity peaks near T_l qualitatively similar to those predicted by our model and shown in Fig. 2. The area under these peaks is the latent heat of melting. Zhu and Dash attribute the vanishing latent heat as the film thins to be due to the smearing out of the solid-liquid interface. In our model (where the interface is discontinuous, in accordance with the well-known Gibbs construction) the effect is attributed instead to repulsion between the three interfaces. However, the repulsion of interfaces is really the way in which our model expresses the fact that free-energy considerations favor a gradual change in density. The two interpretations are therefore qualitatively similar.

As pointed out above, the temperatures at which these peaks appear in thick films are not predicted correctly by our model, nor by that of Zhu and Dash. This discrepancy may be due to some as-yet undetermined error in the values of parameters, such as the various ΔC_3 's.

By contrast, in the methane/graphite system, where stratification does not occur, the analogous calculation, which predicts the slope of the multilayer melting curve, agrees extremely well with experiment.⁴ However, in this case the model does not predict the observed vanishing of the latent heat of melting in thin films. The reason is clearly that in this case the physics of melting in a thin film is not adequately represented by a bulklike continuum slab model.²⁷ This is precisely why we have pursued this part of the problem experimentally.

The results of our NMR measurements indicate that melting in methane/graphite continues to occur below the film thickness at which the latent heat vanishes. This observation strongly suggests that methane/graphite is an ideal system in which to study the evolution of melting from 2D to 3D behavior. Unfortunately, for technical reasons the present measurements lack both the temperature resolution and the clarity of interpretation, i.e., the relation between T_2 and other properties needed for such a study. It is clear, however, that the multilayer melting curve—which is also a prewetting curve since it meets bulk coexistence at a triple-point dewetting transition—has a critical point at about four layers, then extends to thinner films possibly as a higher-order phase transition.

Since melting in 3D is always a first-order phase transition, it seems reasonable to believe that the higher-order character of the transition below four layers reflects intrinsically 2D behavior. We are confident that further experimental study of this system will be of great importance.

ACKNOWLEDGMENTS

The authors would like to thank Bob Housley for helpful discussions during the progress of this work. This work was supported by Department of Energy (DOE) Contract No. DE-FG03-85ER45192.

-
- ¹M. Bienfait, J. L. Seguin, J. Suzanne, E. Lerner, J. Krim, and J. G. Dash, *Phys. Rev. B* **29**, 983 (1984).
- ²A complete review of the literature on wetting is given by S. Dietrich, in *Phase Transitions and Critical Phenomena*, edited by C. Domb and J. Lebowitz (Academic, New York, 1988), Vol. 12.
- ³J. J. Hamilton and D. L. Goodstein, *Phys. Rev. B* **28**, 3838 (1983); D. L. Goodstein, J. J. Hamilton, M. J. Lysek, and G. Vidali, *Surf. Sci.* **148**, 187 (1984).
- ⁴M. J. Lysek, M. S. Pettersen, and D. L. Goodstein, *Phys. Lett. A* **115**, 340 (1986); M. S. Pettersen, M. J. Lysek, and D. L. Goodstein, *Surf. Sci.* **175**, 141 (1986).
- ⁵D.-M. Zhu and J. G. Dash, *Phys. Rev. Lett.* **60**, 432 (1988).
- ⁶D.-M. Zhu and J. G. Dash, *Phys. Rev. Lett.* **57**, 2959 (1986).
- ⁷M. Bienfait, *Europhys. Lett.* **4**, 79 (1987).
- ⁸R. Pandit and M. E. Fisher, *Phys. Rev. Lett.* **51**, 1772 (1983); C. Ebner, *Phys. Rev. B* **28**, 2890 (1983).
- ⁹J. M. Kosterlitz and D. J. Thouless, *J. Phys. C* **6**, 1181 (1973); D. R. Nelson and B. I. Halperin, *Phys. Rev. B* **19**, 2457 (1979); A. P. Young, *ibid.* **19**, 1855 (1979).
- ¹⁰J. Frenkel, *Kinetic Theory of Liquids* (Oxford University, London, 1949); G. D. Halsey, Jr., *J. Chem. Phys.* **16**, 931 (1948); T. L. Hill, *ibid.* **17**, 590 (1949).
- ¹¹G. An and M. Schick, *Phys. Rev. B* **37**, 7534 (1988).
- ¹²P. G. deGennes, *J. Phys. (Paris) Lett.* **42**, 1377 (1981).
- ¹³L. D. Landau and E. M. Lifshitz, in *Statistical Physics*, 3rd ed., edited by E. M. Lifshitz, L. P. Pitaevskii, J. B. Sykes, and M. J. Kearsley (Pergamon, Oxford, 1982), Pt. I.
- ¹⁴J. Krim and J. G. Dash, *Surf. Sci.* **162**, 421 (1985).
- ¹⁵G. Vidali and M. W. Cole, *Surf. Sci.* **110**, 10 (1981).
- ¹⁶W. G. Clark, *Rev. Sci. Instrum.* **35**, 316 (1964).
- ¹⁷A. Abragam, *Principles of Nuclear Magnetism* (Oxford University, Oxford, 1963), Chap. III.
- ¹⁸M. S. Pettersen and D. L. Goodstein, *Surf. Sci.* **209**, 455 (1989).
- ¹⁹G. A. deWit and M. Bloom, *Can. J. Phys.* **42**, 986 (1965).
- ²⁰P. H. Oosting and N. J. Trappeniers, *Physica* **51**, 395 (1971).
- ²¹D. L. Husa, D. C. Hickernell, and J. E. Piott, in *Monolayer and Submonolayer Helium Films*, edited by J. G. Daunt and E. Lerner (Plenum, New York, 1973), p. 133.
- ²²B. Robertson, *Phys. Rev.* **151**, 273 (1966).
- ²³J. G. Dash and R. D. Puff, *Phys. Rev. B* **24**, 295 (1981).
- ²⁴J. H. Quateman and M. Bretz, *Phys. Rev. B* **29**, 1159 (1984); H. K. Kim, Q. M. Zhang, and M. H. W. Chan, *ibid.* **34**, 4699 (1986).
- ²⁵F. F. Buff, R. A. Lovett, and F. H. Stillinger, Jr., *Phys. Rev. Lett.* **15**, 621 (1965); M. W. Cole, *J. Chem. Phys.* **73**, 4012 (1980).
- ²⁶D.-M. Zhu and J. G. Dash, *Phys. Rev. B* **38**, 11 673 (1988).
- ²⁷Many other features of the methane/graphite system are reproduced in a recent analysis of the Potts lattice-gas model by M. W. Conner and C. Ebner, *Phys. Rev. B* **36**, 3683 (1987).